Euler Buckling of Individual SiGe/Si Microtubes

L. Zhang[*], L.X. Dong[**], D.J. Bell[**], B.J. Nelson[**], C. Schönenberger[***] and D. Grützmacher[*]

[*]Laboratory for Micro- and Nanotechnology, Paul Scherrer Institute, CH-5232 Villigen-PSI, Switzerland
li.zhang, detlev.gruetzmacher@psi.ch
[**]Institute of Robotics and Intelligent Systems, ETH Zurich, CH-8092 Zurich, Switzerland
ldong, dbell, bnelson@ethz.ch
[***] Institut für Physik, University of Basel, Klingelbergstrasse 82, CH-4056 Basel, Switzerland
christian.schoenenberger@unibas.ch

ABSTRACT

We present a new technique to investigate the mechanical stability of freestanding rolled-up SiGe/Si microtubes based on nanorobotic manipulation. By applying this technique, the microtubes can be cut and subsequently picked up from the original substrate to examine their mechanical properties in free space or to assemble them into micro-/nanoelectromechanical systems (MEMS/NEMS). Individual SiGe/Si microtubes show typical Euler buckling when the compressive load is larger than the critical load. The experiments show that SiGe/Si microtubes rolled-up by 1.6 turns have similar mechanical stability to ideal seamless tubes, though the former ones contain seams on the walls.

Keywords: microtube, nanorobotic manipulation, mechanical stability, Euler buckling,

1 INTRODUCTION

New strategies to fabricate semiconducting micro-and nanotubes have been introduced in recent years by employing the self-scrolling technique, which is based on the strain relieving behavior of a semiconductor bilayer after it is detached from a substrate [1-4]. These tubes have wall thicknesses in the nanometer range, high aspect ratios of length to diameter, and atomically smooth surfaces. They can be fabricated in a controlled fashion. Here we investigate their mechanical properties, which are significant for many applications such as micro-injection needles, probes and force sensors [2, 5].

The characterization of such tubes has been a challenge, because the complex manipulation of micro- and nanoscale objects in free space is required. The handling techniques required are beyond the capability of atomic force microscopes (AFM). Previous experiments show that the buckling test in free space [6] is an ideal way to investigate the mechanical stability of nanotubes undergoing compressive loading. Different buckling modes have been found when the length and diameter of the nanotubes are varied [6-8]. When a thin-walled tube has a slenderness ratio larger than 100 [9], uniaxial compression results in Euler buckling; whereas for a thin-walled tube with a smaller slenderness ratio, i.e. less than 100, the compressive load leads to shell buckling. Euler buckling, which is a non-destructive technique, has proven effective in the mechanical characterization of single carbon nanotubes using nanorobotic manipulation [6]. In the experiments presented in this study the buckling test was applied to investigate the compression instabilities of individual SiGe/Si microtubes.

2 EXPERIMENTS

2.1 Fabrication of SiGe/Si microtubes

The SiGe/Si bilayers were epitaxially grown on low-doped 4 inch Si (001) wafers by ultrahigh vacuum chemical vapor deposition (UHV-CVD) at 550ºC. The thickness of the layers was below the critical thickness in order to maintain the elastic strain in the SiGe film. To selectively etch the Si substrate under the SiGe/Si heterostrucutres, the SiGe/Si bilayer was heavily boron doped to a level of about $1x10^{20}cm^{-3}$. For electron beam lithography, a double layer resist containing a 15 nm Cr layer and a 100 nm thick spin-coated polymethylmethacrylate (PMMA) layer were used. After developing the PMMA film, reactive ion etching (RIE) with Cl_2 and CO_2 gas was performed to transfer the pattern from the PMMA to the Cr layer. Next, RIE was applied using a mixture of SF_6, CHF_3 and O_2 gas to transfer the pattern into the SiGe/Si bilayer. The initial planar films consist of SiGe/Si/Cr layers with a thickness of 11/8/15 nm, respectively, and about 40% Ge in the SiGe layer. The Cr layer was removed by RIE before the selective wet etching of the substrate under the patterned bilayer was applied.

To fabricate SiGe/Si microtubes, the samples were etched in 3.7% NH_4OH aqueous solution at room temperature (300K). The main advantages of using NH_4OH-H_2O is that it does not incorporate alkaline ions which can contaminate CMOS integrated circuits, it is not toxic, and it has a better selectivity for p-doped SiGe/Si bilayers compared to KOH [10-11]. Finally, the samples were dried in a supercritical drier to eliminate the impact of the capillary force [12].

The as grown p-type SiGe/Si bilayer grown on the Si substrate is composed of the unstrained Si layer and the compressively strained SiGe layer. When the SiGe/Si bilayer is detached from the substrate the compressive strain of the SiGe layer will initiate coiling of the bilayer and a portion of the internal stress will relax. The relaxation of the SiGe film induces tensile strain in the p-doped Si layer. The pair of opposite forces (F_1 and F_2) will generate a bending moment to coil the SiGe/Si bilayer, as shown schematically in Fig. 1a. Fig. 1b shows the mesa pattern used to fabricate SiGe/Si microtubes. The freestanding microtubes gathered from this pattern are fixed with one of their ends to the Si substrate, as shown in Fig.1c. The scrolling direction is governed by the anisotropy of Young's modulus, preferring coiling along the [100] directions, however, this can be modified using anisotropic underetching effects [13].

In the experiments, the width of the stripe w was increased from 3.6 μm to 12.3 μm in steps of 1.2 μm to fabricate microtubes with different numbers of turns. The SiGe/Si microtubes were inspected with a Zeiss SUPRA 55VP field emission scanning electron microscopy (FESEM).

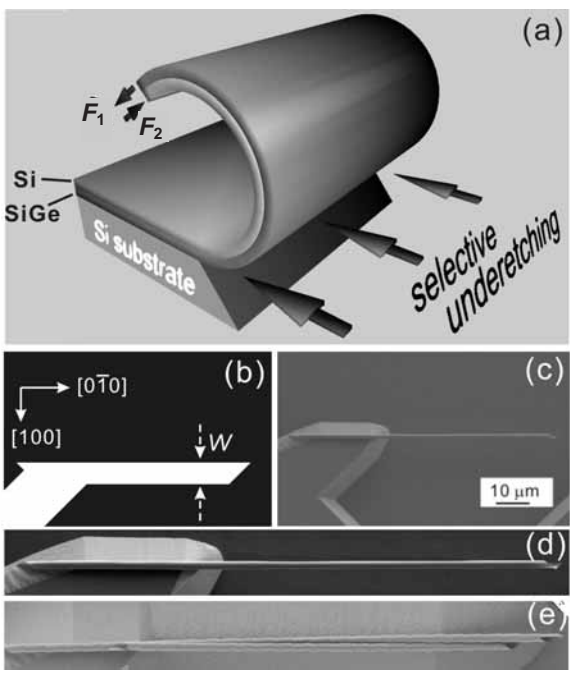

Figure 1: (a) Schematic drawing of rolling of a SiGe/Si bilayer after selective underetching of the Si substrate. (b) The initial mesa pattern used to fabricate freestanding SiGe/Si microtubes. The main scrolling directions of the bilayer are [100] and [-100]. (c) FESEM image of a freestanding SiGe/Si microtube. (d) Magnified view of the image c. (e) Freestanding "double barrel" tubes.

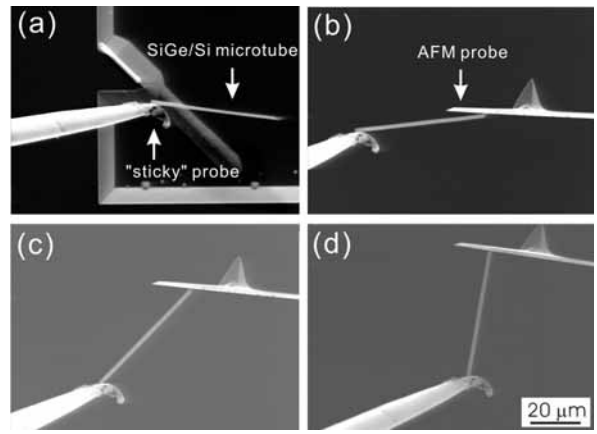

Figure 2: Nanorobotic manipulation of a freestanding SiGe/Si microtube. (a) Cutting and picking up, (b) Placing, (c-d) Rotating. All four SEM images have the same scale bar.

2.2 Nanorobotic manipulation

Nanorobotic manipulation has been successfully applied to freestanding 3D micro- and nanostructures such as SiGe/Si/Cr helices and Si/Cr nano-spirals [14-15] to study their mechanical properties. Here a similar approach was employed to test the mechanical stability of individual SiGe/Si microtubes. A nanorobotic manipulator (MM3A^{TM} from Kleindiek) holding a tungsten probe (Picoprobe T-1-10-1mm) was installed inside a Zeiss DSM962 scanning electron microscope (SEM). A "sticky" probe is prepared by dipping the tip of the probe into double-sided SEM silver conductive tape (Ted Pella, Inc.). This sticky probe is used to cut individual freestanding SiGe/Si microtubes from the substrate (Fig. 2a). The sticky probe was attached to the microtube close to the place were the tube is fixed to the substrate, and then the probe is moved sidewise to break it off from the substrate (see Fig. 2a.). Next the micromanipulator is used to bring the microtube into contact with the backside of an AFM cantilever and to maneuver it to a position so that its axis is perpendicular to the AFM cantilever. Thus, the tube is in an upright position between the cantilever and the probe required for the buckling test. The manipulation sequence is shown in Fig. 2a-d. The tube is shown attached to a ball-like joint at the sticky probe. At the other end of the microtube, the contact between the AFM cantilever and the microtube depends on the backside of the AFM cantilever. When the AFM cantilever has a smooth backside the tube stands freely. To fix the tube to the cantilever, a second type of AFM cantilever with a pyramid hole at the backside has been used. The latter configuration is favorable, because it becomes possible to adjust the angle between the tube and the manipulator probe, as well as between the tube and the cantilever to 90 degrees. Moreover, the microtube will not readily slide on the backside of the AFM cantilever during the buckling test. This buckling test is performed by

pushing the "sticky" probe along the tube axis. The microtube is subject to uniaxial compressive stress and deflects the AFM cantilever with a known spring constant. The deflection of the AFM cantilever measures the compressive force applied to the longitudinal axes of the tube from which the load and the stress on the microtube can be obtained.

3 RESULTS AND DISCUSSION

The pre-patterned SiGe/Si bilayer was scrolled into freestanding tubes with a diameter d of about 1.25 μm (Fig. 1c), close to the calculated value of 1.22 μm [16]. Since the bilayer begins coiling from both sides of the mesa stripe simultaneously, i.e. along the [100] and [-100] direction, the width of the stripe w should be appropriately selected. According to our results, when the width of the stripe w is less than 1.6 times of the tube circumference, i.e. $1.6\pi d$, a single freestanding tube can be fabricated, as shown in Fig. 1c-d. For $w > 1.6\pi d$, two parallel tubes as shown in Fig. 1e are formed. By increasing the width of the mesa line each of the two tubes will contain several turns. Our observations indicate that the walls of tubes with more than 3 turns may stick together to form a closed tube. The length of the microtubes for the buckling test was typically 62 μm to 50 μm. The slenderness ratios of these rolled-up tubes are between 140 and 114, calculated by ideal seamless tubes with the same diameter (1.25 μm), wall thickness (19 nm) and length (62-50 μm).

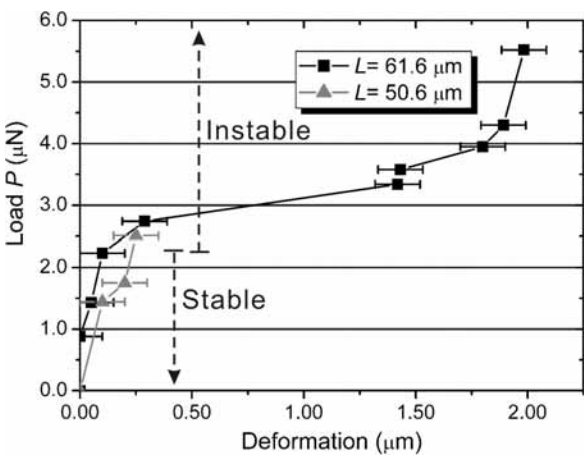

Figure 3: Force versus displacement results for a 61.6 μm and a 50.6 μm long SiGe/Si microtubes. The stable and instable region of the 61.6 μm long tube is marked in the image.

Fig. 3 shows the dependence of the deformation of the microtube on the applied force for a SiGe/Si microtube with a length of 61.6 μm. The deformation of the tube is measured as the distance between the probe and the AFM cantilever, which decreases during the buckling test. Three regimes can be identified. Initially, the load increases linearly with very small displacement; the microtube is in stable equilibrium and is straight. In the second regime the curve becomes flat. The sudden drop of the slope indicates that the tube is beginning to buckle [17]. Finally, in the third regime, the slope becomes steep again while the wall of the tube is severely bent. A typical Euler buckled microtube is shown in Fig. 4a where the bending of the tube is clearly visible. A further increase of the load leads to local deformation of the tube and finally to mechanical fracture of the microtube.

The kink point of the curve between the first and the second stage represents the neutral equilibrium of the microtube. The corresponding load is defined as the critical load (P_{cr}). As shown in Fig. 3, a value of the critical load close to 2.2 μN is determined for a 61.6 μm long 1.6-turn SiGe/Si microtube. The critical stress (σ_{cr}) can be expressed by:

$$\sigma_{cr} = P_{cr} / A \tag{1}$$

where A is the cross sectional area of the tube. The critical stress is worked out as 18.4 MPa. It should be noted that bilayers scrolled into incomplete tubes, e.g. ¾ of a turn, reveal a critical stress approximately one order of magnitude smaller than that of the films scrolled by 1.6 turns. For a microtube with a length of 50.6 μm and the same diameter and wall thickness, the tube is straight up to a compressive load of 2.5 μN. The stress in this microtube is 20.9 MPa. The displacement-load curve is presented in Fig. 2 with gray lines. In this experiment a cantilever with a flat back surface has been used, hence this tube slipped away from the back side of AFM cantilever before it apparently buckled.

According to the Euler's formula [17], the critical load can be expressed as:

$$P_{cr} = \frac{\pi^2 EI}{L_{eff}^2} \tag{2}$$

in which EI is the flexural rigidity, and L_{eff} is the effective length of the tube ($L_{eff} = 2L$, for hinged-fixed condition and $L_{eff} = L$ for hinged-free condition [17]). Using this formula the calculated critical load for an ideal seamless Si mictotube with 61.6 μm length and hinged-fixed condition is about 1.23 μN. Here the Young's modulus of Si from bulk material [18] and a Si tube with a diameter of 1.25 μm and a wall width of 19 nm has been assumed. A 1.6 turn rolled-up tube is approximated as a combination of an idea tube and a 0.6 turn tube, so the cross sectional area is the sum of a thin circular ring and a thin circular arc. For this 1.6 turned ideal tube the critical load is calculated to be 2.0 μN. This result indicates that the mechanical stability of a scrolled microtube, with 1.6 turns, is similar to a seamless tube. Thus, the critical load and the flexural rigidity (EI) of

the scrolled microtube having more than 1.6 turns can be approximated by an ideal seamless tube.

The deviation of the real flexural rigidity of a scrolled microtube and the calculated value from the ideal tube might result from the difference of the moment of inertia of cross sectional area *I*. For an ideal seamless tube, *I* can be calculated as $I = \frac{\pi}{8} d^3 t$ when $d << t$ [17], where *d* and *t* are the diameter and wall thickness of the tube. However, the multi-turn rolled-up microtube has a seam along the tube axis.

In the rolled up bilayer the two ends of the rolled sheet do not bond together to form a seamless tube. However, when those ends overlap sufficiently the tubes become quite stable. Surprisingly, the microtubes do not open along the seam when the axial compressive force is larger than the critical load. Additionally, the microtubes exhibit an excellent ability to recover from the post-buckling stage to their initial straight shape, as shown in Fig. 4a and Fig. 4b. Moreover, in cycling the experiment the critical load remained unchanged after the microtube recovered from the buckled state. This implies that the microtube is elastically deformed and no permanent changes occur in the SiGe/Si crystalline structure, even after it has been exposed to the instable equilibrium state. An interesting observation is that in the third regime, the microtube becomes stiffer again (see Fig. 2). This may be due to the increase of the moment of inertia of the cross sectional area of the microtube. When the microtube is heavily buckled, the cross sectional shape is no longer ring-like. Also, in this stage the neighboring walls of the tube may interact with each other leading to a reinforcement of the stiffness of the tube. When the microtube is strongly buckled, the internal (compression) side walls of the tube may open locally, which leads to highly localized stress. If the applied load is higher than the maximum value, the tube will be destroyed.

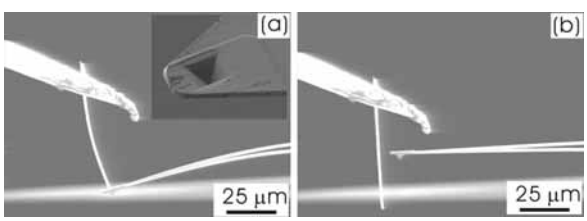

Figure 4: (a) Post-buckling state of a 61.6 μm long SiGe/Si tube. (b) The tube recovered from the axial compressive load. Inset: An AFM cantilever with a hole on the backside.

4 CONCLUSIONS

Euler buckling has been experimentally observed in SiGe/Si microtubes when they are subjected to axial compressive load by nanorobotic manipulation. The flexural rigidity of the scrolled SiGe/Si microtube, which has more than 1.6 turns, is close to the ideal seamless tube. The self-scrolled SiGe/Si microtubes show no ductility and excellent elastic recovery from the post-buckling state is observed. The manipulation technique developed has proven to be a suitable approach for characterizing the mechanical properties of these self-scrolled semiconductor micro- and nanostructures.

ACKNOWLEDGEMENT

The authors thank Eugen Deckardt and Anja Weber (Paul Scherrer Institute) for their technical support. This work is supported by the Swiss National Science Foundation (SNF) and the ETH-Zurich.

REFERENCES

[1] V.Ya. Prinz, V.A. Seleznev, A.K. Gutakovsky, A.V. Chehovskiy, V.V. Preobrazhenskii, M.A. Putyato, and T.A. Gavrilova, Physica E 6, 828, 2000.
[2] O.G. Schmidt and K. Eberl, Nature 410, 168, 2001.
[3] S.V. Golod, V.Ya. Prinz, V.I. Mashanov and A.K. Gutakovsky, Semicond. Sci. Technol. 16, 181, 2001
[4] L. Zhang, S.V. Golod, E. Deckardt, V. Prinz and D. Grützmacher, Physica E 23, 280, 2004.
[5] A.V. Prinz and V.Ya. Prinz, Surf. Sci. 532, 911, 2003.
[6] L.X. Dong, F. Arai, and T. Fukuda, IEEE/ASME Trans. Mechatronics 9, 350, 2004.
[7] J.F. Waters, P.R. Guduru, M. Jouzi, J.M. Xu, T. Hanlon, and S. Suresh, Appl. Phys. Lett. 87, 103109, 2005.
[8] A. Cao, P.L. Dickrell, W.G. Sawyer, M.N. Ghasemi-Nejhad, and P.M. Ajayan, Science 310, 1307, 2005.
[9] S.P. Timoshenko and J.M. Gere, Theory of elastic stability, New York, Mcgraw-hill, 1985
[10] U. Schnakenberg, W. Benecke, and B. Löchel, Sens. Actuators, A21-A23, 1031, 1990.
[11] U. Schnakenberg, W. Benecke, B. Löchel, S. Ullerich, and P. Lange, Sens. Actuators A25-27, 1, 1991.
[12] V. Seleznev, H. Yamaguchi, Y. Hirayama and V.Ya. Prinz, Jap. J. Appl. Phys. 42, 791. 2003.
[13] S.V. Golod, V.Ya. Prinz, P. Wägli, L. Zhang, O. Kirfel, E. Deckhardt, F. Glaus, C. David, and D. Grützmacher, Appl. Phys. Lett. 84, 3391, 2004.
[14] D. Bell, Y. Sun, L. Zhang, L.X. Dong, B. Nelson and D. Grützmacher, Sens. Actuators A, in press.
[15] L. Zhang, L.X. Dong, D. Bell, B. Nelson, C. Schönenberger, and D. Grützmacher, Microelectron. Eng., in press.
[16] M. Grundmann , Appl. Phys. Lett. 83, 2444, 2003.
[17] J.M. Gere, Mechanics of materials, Belmont, US 2004.
[18] J.J. Wortman and R.A. Evans, J. Appl. Phys. 36(1), 153, 1965.